The Canadian Mineralogist
Vol. 36, pp. 49-66 (1998)

THE MAFIC MINERALS OF THE FALCON ISLAND ULTRAPOTASSIC PLUTON, LAKE OF THE WOODS, ONTARIO: PROGRESSIVE REDUCTION DURING FRACTIONATION

JOHN A. AYER[1]

Ontario Geological Survey, 933 Ramsey Lake Road, Sudbury, Ontario P3E 6B5

ABSTRACT

The Falcon Island complex is an ultrapotassic pluton with a U–Pb age of 2695 ± 3 Ma intruding the Lake of the Woods greenstone belt in the Wabigoon Subprovince of the Superior Province, in western Ontario. It consists of nepheline-bearing alkali feldspar syenite and alkali feldspar melasyenite with lesser amounts of clinopyroxenite, monzodiorite, and peraluminous alkali feldspar syenite. The magma evolved with increasing $P(H_2O)$, as indicated by clinopyroxene cores mantled by hornblende, and hypersolvus perthitic alkali feldspar phenocrysts followed by subsolvus interstitial plagioclase, alkali feldspar and nepheline. An "aegirine-enrichment trend" is evident in the clinopyroxene as progressive depletion in Mg and Ca, and enrichment in Fe and Na (both as zoning in individual grains and in the successively fractionated units). Decreasing $Fe^{3+}/(Fe^{2+} + Fe^{3+})$ accompanied by increasing Fe/(Fe + Mg), Ti, and ^{IV}Al contents of the biotite of the fractionated rock units indicates progressive reduction and Al enrichment of the magma with fractionation. A spatial and genetic linkage of gold mineralization to oxidized alkaline intrusions has been proposed on the basis of mineral chemical studies from the Abitibi Subprovince. The lack of spatially associated gold mineralization with the progressively reduced Falcon Island pluton, despite its proximity to a potentially favorable zone of deformation, supports this hypothesis.

Keywords: Falcon Island pluton, Wabigoon belt, syenite, clinopyroxene, amphibole, biotite, feldspars, fractional crystallization, ultrapotassic suite, Lake of the Woods greenstone belt, Ontario.

SOMMAIRE

Le complexe plutonique de l'île Falcon, ultrapotassique, a été mis en place il y a 2695 ± 3 Ma (âge U–Pb) dans la ceinture de roches vertes dite Lake of the Woods, dans la sous-province de Wabigoon, province du Supérieur, dans la partie occidentale de l'Ontario. La suite est constituée de syénite à feldspath alcalin contenant néphéline, ainsi que des mélasyénites, avec des quantités moindres de pyroxénite, monzodiorite, et syénite peralumineuse à feldspath alcalin. Le magma a évolué avec une augmentation de $P(H_2O)$, comme en témoigne les coeurs de clinopyroxène avec une bordure de hornblende, ainsi que les phénocristaux de feldspath alcalin perthitiques, et donc à caractère hypersolvus, suivis d'un assemblage subsolvus interstitiel de plagioclase, feldspath alcalin et néphéline. Le clinopyroxène fait preuve d'un enrichissement progressif en aegirine à mesure que diminuent les teneurs en Mg et Ca, et qu'augmentent les teneurs en Fe et Na (démontré soit par zonation dans un seul cristal, soit en considérant le clinopyroxène de l'ensemble des unités). Une diminution du rapport $Fe^{3+}/(Fe^{2+} + Fe^{3+})$ accompagnée d'une augmentation de Fe/(Fe + Mg) et des teneurs en Ti et ^{IV}Al de la biotite des unités les plus évoluées indiquent une réduction progressive du magma et son enrichissement progressif en Al. Un lien dans l'espace et dans le temps des plutons oxydés avec la minéralisation en or a été proposé à la lumière des études de la composition des minéraux primaires des plutons dans la sous-province de l'Abitibi. L'absence de telle minéralisation près du pluton de l'île Falcon, plus réduit dans ses termes évolués, ceci malgré la proximité d'une zone de déformation jugée favorable, vient étayer cette hypothèse.

(Traduit par la Rédaction)

Mots-clés: pluton de l'île Falcon, ceinture de Wabigoon, syénite, clinopyroxène, amphibole, biotite, feldspaths, cristallisation fractionnée, suite ultrapotassique, ceinture de roches vertes, Lake of the Woods, Ontario.

INTRODUCTION

Precambrian alkaline magmatism is uncommon (Corriveau & Gorton 1993, Blichert-Toft *et al.* 1996), and well-documented accounts of mineral chemistry of Archean ultrapotassic plutons are mostly restricted to the Abitibi Subprovince of the Superior Province (Ben Othman *et al.* 1990, Laflèche *et al.* 1991, Rowins *et al.* 1993). In the Phanerozoic, ultrapotassic, potassic and shoshonitic suites associated with calc-alkaline magmatism are restricted to arc environments (Foley *et al.* 1987, Wheller *et al.* 1987). In the Abitibi Subprovince, coeval, late-tectonic, alkaline volcanic suites of the Timiskaming Group and coeval alkaline

[1] *E-mail address*: ayerjo@epo.gov.on.ca

plutons have important economic implications because of their close spatial and temporal association with gold mineralization (Sinclair 1982, McNeil & Kerrich 1986, Fyon *et al.* 1989, Rock & Groves 1988, Wyman & Kerrich 1989, Robert 1997). The oxidation state of the Abitibi intrusive suites is variable and also considered to play an important role in mineralization (Cameron & Carrigan 1987, Cameron & Hattori 1987, Rowins *et al.* 1991, 1993, Lévesque 1994).

The Falcon Island composite pluton is located in the southern part of the Lake of the Woods greenstone belt, within the Wabigoon Subprovince of the Superior Province in northwestern Ontario (Fig. 1). The pluton was chosen for detailed study because of its ultrapotassic composition, a relatively rare occurrence in the Archean, and its similarity in age and geochemistry to the potassic, shoshonitic metavolcanic units in the Electrum Lake Assemblage, an unconformable, "Timiskaming-like" sedimentary basin in the northern part of the belt. Both the pluton and the Electrum Lake Assemblage are considered to be derived from a mantle wedge formed in the late stages of a mature island arc or a continental arc setting of Neoarchean age (Ayer & Davis 1997).

Comparison of the mineral chemistry of the Falcon Island pluton with that of other syenitic complexes, including oxidized complexes in the Kirkland Lake gold camp, provides insight into the geodynamic processes associated with gold mineralization in the Neoarchean. Another paper, further documenting the lithochemical trends and the Nd and Pb isotopic characteristics of the pluton and the supracrustal suites of the Lake of the Woods greenstone belt, is in progress.

Regional Context

The Falcon Island complex intrudes tholeiites of the Lower Keewatin Assemblage (2738 ± 2 Ma) and calc-alkaline metavolcanic rocks, tholeiitic to komatiitic metavolcanic rocks and turbiditic metasedimentary rocks of the Upper Keewatin Assemblage (2723 to 2712 Ma: Ayer & Davis 1997) (Fig. 1). Plutonic rocks of the Lake of the Woods greenstone belt have been subdivided into three groups: 1) predeformation intrusions, including synvolcanic stocks and early tonalite and granodiorite units within the batholiths (2727 to 2717 Ma), 2) syndeformation stocks and the late granitic phases within the batholiths (2711 to 2708 Ma), and 3) late kinematic granitic stocks and the alkaline complexes (including the Falcon Island pluton) (2700 to 2695 Ma).

Gold mineralization is widespread in zones of ductile deformation transecting the Lake of the Woods greenstone belt. Gold deposits with sufficient grade and tonnage to be economic appear to be restricted to the western part of the belt, where they have a "porphyry copper" association coeval in timing, with metal zonations and alteration assemblages in proximity to syndeformation, calc-alkaline plutons (Davis & Smith 1991). There is no evidence of gold mineralization spatially associated with the Falcon Island pluton, despite its proximity to the southern branch of the Pipestone–Cameron deformation zone, a potentially favorable system of faults that host gold mineralization 20 km northeast of the pluton (Ayer & Buck 1989, Ayer 1991).

The Falcon Island Pluton

The Falcon Island plutonic complex is the largest alkaline intrusion in the Lake of the Woods greenstone belt. It was mapped and described by Ayer (1991). U–Pb isotope analyses of titanite from an alkali feldspar syenite border phase indicates an age of crystallization of 2695 ± 3 Ma (Ayer & Davis 1997). This age is similar to the documented ages of other events of alkaline magmatism in the western Wabigoon Subprovince, *e.g.*, the Jackfish Lake pluton (2696 Ma: Sutcliffe *et al.* 1990), the Taylor Lake stock (2695 Ma: Davis *et al.* 1982) and coeval shoshonitic volcanic rocks in the Electrum Lake Assemblage in the northern part of the Lake of the Woods greenstone belt (Ayer & Davis 1997).

The rocks of the complex (Fig. 2) were classified in the field according to IUGS nomenclature on the basis of the relative proportions of alkali feldspar and plagioclase, as indicated by staining of all hand specimens (Ayer 1991). Subsequent electron-microprobe analysis of the minerals indicates the plagioclase is dominantly sodic ($An_{<5}$) and thus should be included with the alkali feldspar in the IUGS classification (Streckeisen 1976). Thus field-classified monzodiorites and syenites that have contents of ferromagnesian minerals in excess of 15% are herein reclassified as feldspathoid-bearing alkali feldspar melasyenites. The field-classified monzonites that have ferromagnesian mineral contents less than 15% are reclassified as feldspathoid-bearing alkali feldspar syenites. The prefix "feldspathoid-bearing" is hereafter dropped for the sake of brevity.

Alkali feldspar melasyenite and alkali feldspar syenite are the most widespread units of the intrusion (Fig. 2). Contacts between the melasyenite and syenite are gradational, but the presence of melasyenite xenoliths in syenite indicates it predates the syenite (Ayer 1991). Alkali feldspar melasyenite is restricted to two zones: (1) an oval core-zone about 8 km by 6 km toward the northeastern end, and (2) a marginal zone up to 3 km wide along the southwestern part of the pluton. Isolated lenticular bodies (up to 3 km by 0.5 km) of monzodiorite and clinopyroxenite occur within the melasyenitic portions of the intrusions. The mafic rock-units have a gradational contact with the melasyenite, and are interpreted as early cumulates.

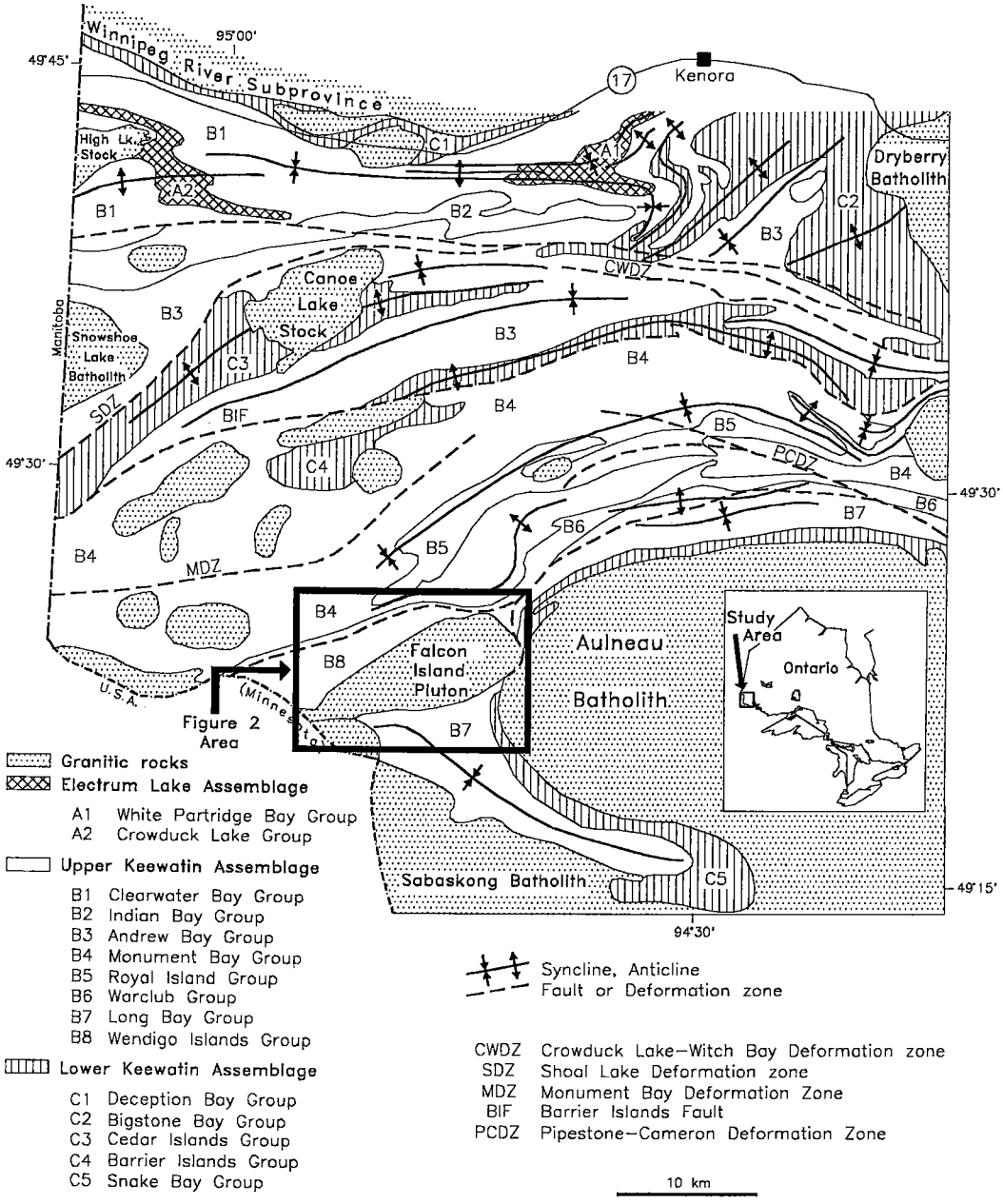

FIG. 1. General geology of the Lake of the Woods greenstone belt (Ayer & Davis 1997).

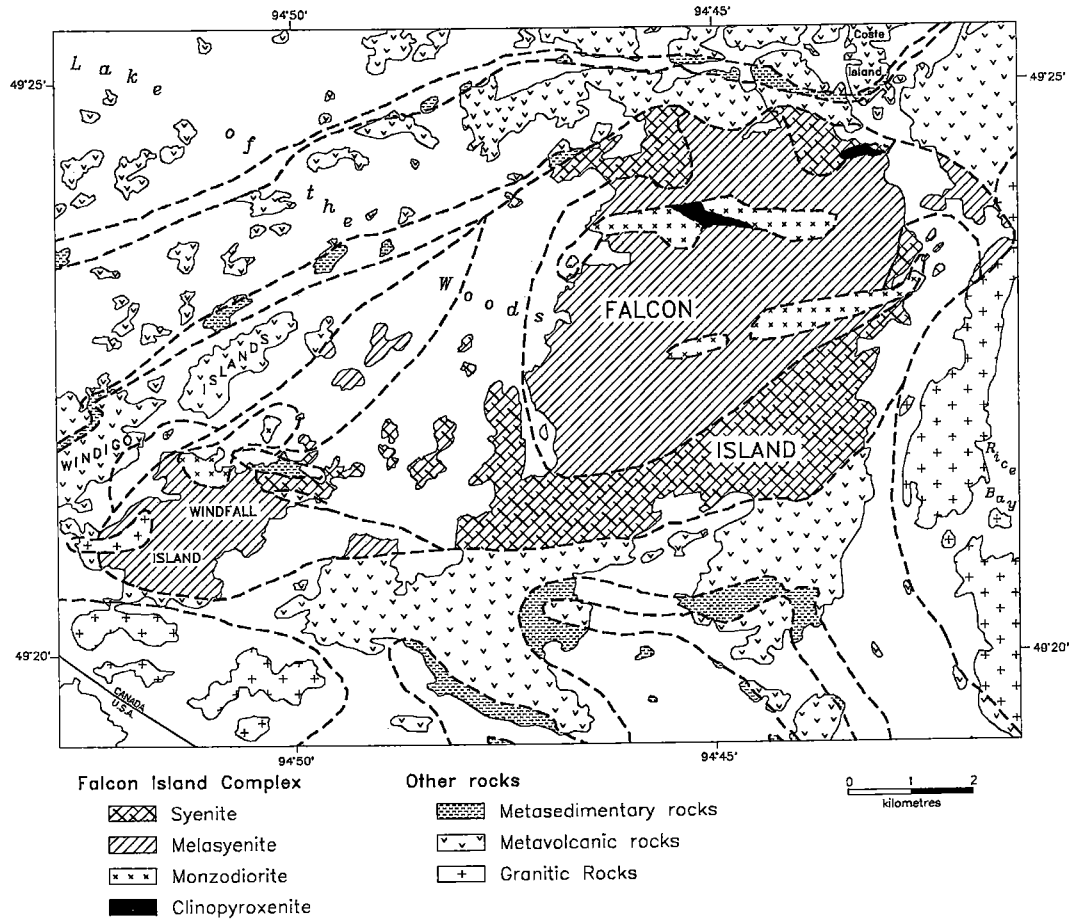

FIG. 2. Geology of the Falcon Island pluton.

The clinopyroxenite is black and consists of medium-grained subhedral clinopyroxene (65%) surrounded by medium-grained anhedral phlogopite (25%) and fine-grained subhedral hornblende (10%). Subhedral magnetite and zircon occur as fine-grained inclusions in clinopyroxene and biotite. The monzodiorite is dark gray and consists of euhedral to subhedral, medium-grained clinopyroxene (50%) surrounded by fine- to medium-grained, anhedral biotite (10%), plagioclase (30%) and perthitic alkali feldspar (5%). Fine-grained, subhedral to euhedral magnetite, apatite, and zircon occur as inclusions in clinopyroxene, biotite and the feldspars. The alkali feldspar melasyenite is pink to red and consists of coarse-grained, tabular microcline phenocrysts, locally aligned in an igneous foliation. Medium- to fine-grained subhedral microperthitic microcline (50–70%), anhedral albite (5–10%), and subhedral to euhedral clinopyroxene (10–20%), rimmed by hornblende (5–10%) and ragged biotite (1–5%), are interstitial to the phenocrysts. Fine-grained subhedral magnetite forms inclusions in the ferromagesian minerals and feldspars. Other accessories include fine-grained, euhedral to anhedral titanite, apatite, and zircon. Fine-grained accessory nepheline (1–5%) occurs as discrete grains with microcline and plagioclase. Subhedral to euhedral epidote and locally andradite are late-stage deuteric overgrowths. The alkali feldspar syenite is pink to gray and is texturally similar to melasyenite. It contains a higher proportion of discrete albite grains (10–20%) relative to microperthitic microcline (60–70%), and a higher proportion of biotite (5–10%) relative to clinopyroxene (1–5%) and amphibole (1–5%). Accessory minerals may include nepheline, magnetite, titanite, apatite and zircon. Replacement minerals may include epidote, andradite

TABLE 1. WHOLE ROCK COMPOSITIONS, FALCON ISLAND PLUTON

Rock Unit	pyroxenite	monzodiorite	melasyenite	melasyenite	syenite	syenite	syenite
Sample #	88-182	88-195	93-32	93-33	88-190	93-31	88-261
SiO_2	46.7	46.6	52.1	56.2	55.6	55.4	59.7
TiO_2	0.66	1.28	0.97	0.56	0.64	0.48	0.36
Al_2O_3	7.13	12.7	13.7	18.0	19.2	19.8	20.0
Fe_2O_3	8.58	13.7	10.7	5.41	4.75	4.23	3.04
MnO	0.14	0.19	0.19	0.11	0.09	0.10	0.06
MgO	16.7	6.91	4.22	1.82	1.56	1.23	0.66
CaO	13.1	10.1	7.36	3.38	3.23	2.08	1.68
Na_2O	0.89	3.34	2.97	4.23	3.33	5.73	4.13
K_2O	3.04	2.83	5.66	8.44	8.29	8.64	7.73
P_2O_5	0.22	1.27	0.78	0.33	0.45	0.20	0.27
CO_2	0.45	0.20			0.40		0.34
LOI	1.50	0.80	1.00	1.00	1.40	0.75	1.00
Total	98.7	98.7	100.0	99.7	98.5	98.8	98.6
TRACE ELEMENTS							
Cr	1200	161	61	17	18	7	nd
Ni	440	53	18	4	nd	3	nd
Co	51	45	21	9	11	6	5
Sc	28	22	13.9	5.46	4	3.17	2
V	104	243			75		25
Cu	17	58	73	29	22	13	98
Pb	nd	nd	2	10	nd	14	nd
Zn	79	141	102	60	74	46	69
Rb	109	105	92	245	237	289	231
Ba			2820	2380		1590	
Sr	570	2068	2710	2470	1969	1520	2200
CIPW NORMS							
Q	0.0	0.0	0.0	0.0	0.0	0.0	0.8
C	0.0	0.0	0.0	0.0	0.0	0.0	2.5
Or	0.0	17.1	34.2	50.9	50.6	52.3	46.9
Ab	0.0	7.3	13.8	15.2	18.9	12.1	35.9
An	6.7	11.8	7.5	5.3	13.4	2.8	6.8
Ne	4.2	11.7	6.4	11.5	5.6	20.4	0.0
Lc	26.0	0.0	0.0	0.0	0.0	0.0	0.0
Hy	0.0	0.0	0.0	0.0	0.0	0.0	5.0
Ol	22.0	15.0	9.5	4.9	6.7	3.8	0.0
Mt	2.1	3.4	2.6	1.4	1.2	1.1	0.8
Hm	0.0	0.0	0.0	0.0	0.0	0.0	0.0
Il	1.3	2.5	1.9	1.1	1.3	0.9	0.7
Ap	0.5	2.8	1.7	0.7	1.0	0.5	0.6
INDICES							
ASI	0.25	0.47	0.56	0.81	0.94	0.88	1.10
DI	15.7	36.1	54.5	77.6	75.1	84.8	83.6
AI	0.67	0.67	0.80	0.89	0.75	0.95	0.76

Oxides in wt %; traces in ppm; Aluminum Saturation Index (ASI) = molar $Al_2O_3/(CaO+K_2O)$; Differentation Index (DI) = normative Q + Or + Ab + Ne + Ks + Lc; Agpaitic Index (AI) = molar $(Na_2O+K_2O)/Al_2O_3$

and chlorite. Pink to gray peraluminous alkali feldspar syenite contains up to 10% microcline phenocrysts in a fine- to medium-grained groundmass of microcline (50–60%), plagioclase (15–25%), biotite (5–10%) and muscovite (1–5%). Accessories include titanite, apatite and epidote.

Whole-rock compositions of representative samples are presented in Table 1. The analytical techniques utilized are as indicated in Ayer & Davis (1997). Duplicates and standards submitted with the samples indicate that precision and accuracy were within 5% (at 2σ) for values greater than 10 times detection limits. The pluton is silica-undersaturated, as evidenced by the presence of normative nepheline and leucite (Table 1). On the basis of agpaitic indices [A.I.; molar $(Na_2O+K_2O)/Al_2O_3$] of less than unity (Sørensen 1974, Mitchell 1996), the pluton is miaskitic ($0.67 < A.I. < 0.95$). Values of $K_2O > 3$ wt.% and $K_2O/Na_2O > 2$ indicate an ultrapotassic composition. The suite is similar to the Group-III ultrapotassic suites (Foley *et al.* 1987) on the basis of elevated Mg (in the mafic units) and Al contents.

Mineral Assemblages

Analytical and recalculation techniques

Mineral analyses were carried out by wavelength-dispersion X-ray spectrometry on a Cameca electron microprobe at the Geoscience Laboratories of the Ontario Geoservices Centre, Ministry of Northern Development and Mines, Sudbury, Ontario. Operation conditions were set to 15 kV and 20 nA using a beam defocused to approximately 10 μm. Count times varied from 15 to 30 seconds per element for the ferromagnesian minerals, and 10 seconds per element for feldspars and nepheline. Recalculation of pyroxene compositions was based on the scheme of Yoder & Tilley (1962). Iron recalculation to Fe^{2+} and Fe^{3+} was done by charge-balance considerations. Pyroxene nomenclature and site assignments follow current IMA guidelines (Morimoto 1989). The amphibole results were recalculated on an anhydrous basis to a total of 13 cations, excluding Ca, Na, and K, per 23 atoms of oxygen, using the charge-balance method to assign ferrous and ferric iron, and the cations assigned to each site according to IMA guidelines (Robinson *et al.* 1982, Leake *et al.* 1997). Biotite compositions are recalculated to 24 atoms of oxygen and 2 OH groups (Deer *et al.* 1963a). The biotite from three samples was separated using heavy-liquid techniques, and selected by hand-picking using a binocular microscope. These separates were analyzed by wet chemistry to determine ferrous iron content, and the results were utilized to adjust FeO and Fe_2O_3. The biotite – annite – siderophyllite – eastonite rectangle of Deer *et al.* (1963a) is the basis of nomenclature. Feldspars and nepheline compositions were recalculated on the basis of 32 atoms of oxygen. Oxide compositions were not recalculated.

Clinopyroxene

Green pleochroic clinopyroxene occurs in all units except peraluminous alkali feldspar syenite. The clinopyroxene grains are subhedral, with equant to prismatic sections up to 6 mm in length. Zoning is visually evident as variation from a pale green pleochroic core to a slightly darker green rim in all units, with the exception of monzodiorite and clinopyroxenite, which exhibit uniform pale green to pale pink pleochroism. The clinopyroxene from alkali feldspar syenite and melasyenite is typically mantled by magmatic amphibole. Biotite, magnetite, apatite, and titanite may occur as inclusions in clinopyroxene.

Clinopyroxene compositions range from magnesian diopside to aegirine-augite in the various units of the

TABLE 2. CHEMICAL COMPOSITION OF CLINOPYROXENE, FALCON ISLAND PLUTON

Rock Unit	clinopyroxenite		monzodiorite		melasyenite		melasyenite		syenite		syenite	
Sample #	182		195		32		33		190		31	
# of anal.	8	s.d.	11	s.d.	9	s.d.	10	s.d.	8	s.d.	9	s.d.
SiO_2 (wt.%)	53.35	1.14	51.16	0.16	5.25	0.39	5.51	0.80	51.00	0.65	53.70	0.25
TiO_2	0.23	0.28	0.47	0.40	0.64	0.35	0.83	0.10	0.73	0.90	0.56	0.31
Al_2O_3	1.49	0.86	2.98	0.39	3.54	0.80	3.33	0.00	3.90	0.32	3.40	0.45
FeO	4.68	1.40	9.16	0.12	11.50	2.40	1.76	1.51	9.43	0.34	12.60	0.93
Cr_2O_3	0.24	0.25	0.20	0.20	0.40	0.20	0.10	0.20		0.00	0.00	0.00
MnO	0.14	0.70	0.35	0.50	0.39	0.70	0.40	0.20	0.32	0.00	0.40	0.90
MgO	15.54	0.40	12.38	0.21	1.49	1.23	1.82	0.83	11.59	0.26	9.61	0.77
CaO	23.66	0.56	22.25	0.24	21.26	1.20	21.33	0.18	21.78	0.11	19.64	1.97
Na_2O	0.58	0.26	0.91	0.20	1.81	0.48	1.87	0.30	1.82	0.10	2.85	1.13
K_2O					0.30	0.50	0.10	0.20	0.10	0.10	0.20	0.20
Total	99.90	0.17	99.68	0.22	99.49	0.15	99.87	0.22	99.77	0.17	99.44	0.37
Structural formula based on 4 cations and 6 atoms of oxygen.												
TSi (a.p.f.u.)	1.96		1.91		1.89		1.89		1.90		1.89	
TAl	0.04		0.09		0.11		0.11		0.10		0.11	
M1Al	0.02		0.04		0.04		0.03		0.03		0.04	
M1Ti	0.01		0.01		0.02		0.02		0.02		0.02	
M1Fe^{3+}	0.05		0.09		0.16		0.17		0.16		0.25	
M1Fe^{2+}	0.07		0.17		0.18		0.17		0.13		0.15	
M1Cr	0.01											
M1Mg	0.85		0.69		0.59		0.6		0.64		0.54	
M2Fe^{2+}	0.03		0.03									
M2Mn			0.01		0.01		0.01		0.01		0.01	
M2Ca	0.93		0.89		0.86		0.85		0.87		0.79	
M2Na	0.04		0.07		0.13		0.14		0.13		0.21	
Fe/(Fe+Mg)	0.15		0.30		0.37		0.36		0.31		0.43	
Na/(Na+Ca)	0.04		0.07		0.13		0.14		0.13		0.21	
$Fe^{3+}/(Fe^{2+}+Fe^{3+})$	0.33		0.31		0.47		0.50		0.55		0.63	

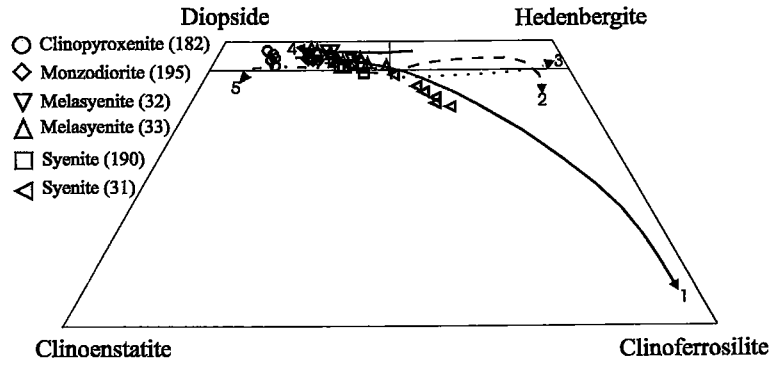

FIG. 3. Compositions of the clinopyroxene from the Falcon Island pluton in terms of the pyroxene quadrilateral (Morimoto 1989). For comparative purposes, trends of crystallization from a number of other differentiated alkaline intrusions are shown: (1) Shonkin Sag laccolith (Nash & Wilkinson 1970), (2) Klokken gabbro–syenite complex (Parsons 1979), (3) Kûngnât syenites (Upton 1960), (4) Baie-des-Moutons syenitic complex, early-group syenites (Lalonde & Martin 1983) and (5) Kirkland Lake suites (Lévesque 1994).

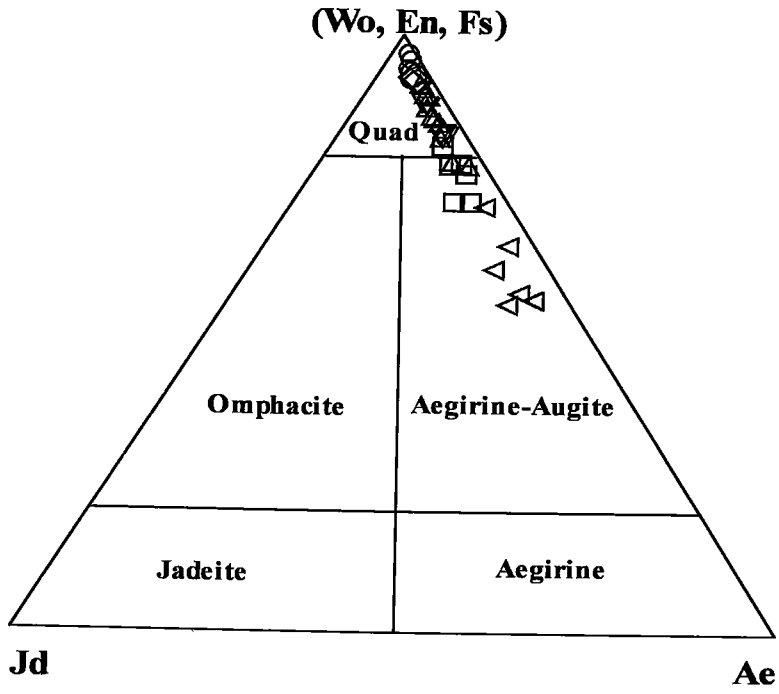

FIG. 4. Compositions of the clinopyroxene in the Falcon Island pluton in the "quad" – jadeite – aegirine plot (Morimoto 1989). Symbols as in Figure 3.

complex. Compositional averages from representative samples are presented in Table 2, as most of the clinopyroxene grains exhibit systematic zoning from core to rim. The degree of variation is indicated by the standard deviations (Table 2) and the positions of the individual compositions on Figures 3, 4 and 5. Intragrain variation from core to rim is magmatic, as indicated by its similarity to the overall differentiation trend of the complex, from early near-end-member diopside in clinopyroxenite to progressively more Fe-rich diopside in monzodiorite and melasyenite, and finally to Fe- and Na-rich and Ca-poor aegirine-augite in syenite (Figs. 3–5). The compositions demonstrate increasing Fe/(Fe + Mg), from 0.15 to 0.43 (Table 2) with fractionation. Inferred $Fe^{3+}/(Fe^{2+} + Fe^{3+})$ values also increase with fractionation (from 0.3 to 0.6), which might normally suggest oxidation. However, McGuire *et al.* (1989) have shown that calculated Fe^{2+} and Fe^{3+} values assuming electrostatic neutrality and the stoichiometry of the low-pressure end-members of Cawthorn & Collerson (1974) are suspect for pyroxene crystallized under higher pressures, the likely environment of crystallization of the pluton.

Clinopyroxenes from differentiated alkaline complexes evolve with a variety of compositional trends. Typically, they evolve toward a more iron-rich composition (LeBas 1962). In many cases, such as the Shiant Isles (Gibb 1973) and the Klokken (Parsons 1979) intrusions, a "hedenbergite-enrichment" trend roughly parallels the diopside – hedenbergite join, indicating extensive substitution of Fe^{2+} for Mg without any significant substitution in the Ca site. In some alkaline intrusions, decreasing or constant Fe/(Fe + Mg) values are evident (*e.g.*, Kirkland Lake and Baie-des-Moutons trends on Fig. 3). This type of trend, caused by incorporation of iron dominantly as Fe^{3+} in oxide phases, leading to a deficiency in Fe^{2+} and substitution of Mg for ferrous iron, is attributed to progressively higher fugacity of oxygen with differentiation (Czamanske & Wones 1973, Lalonde & Martin 1983, Rowins *et al.* 1991, Lévesque 1994). Clinopyroxene compositions from still other alkaline suites exhibit progressive Ca depletion from diopside toward the clinoferrosilite corner of the pyroxene quadrilateral (*e.g.*, Falcon Island and Shonkin Sag trends on Fig. 3). This "aegirine enrichment" trend reflects substitution of $NaFe^{3+}$ for $CaFe^{2+}$ and is evident on Figure 4, as an evolution away from the Ca–Mg–Fe plane of the quadrilateral into the field of aegirine-augite, and on Figure 5 as progressive enrichment in Na and Fe. The

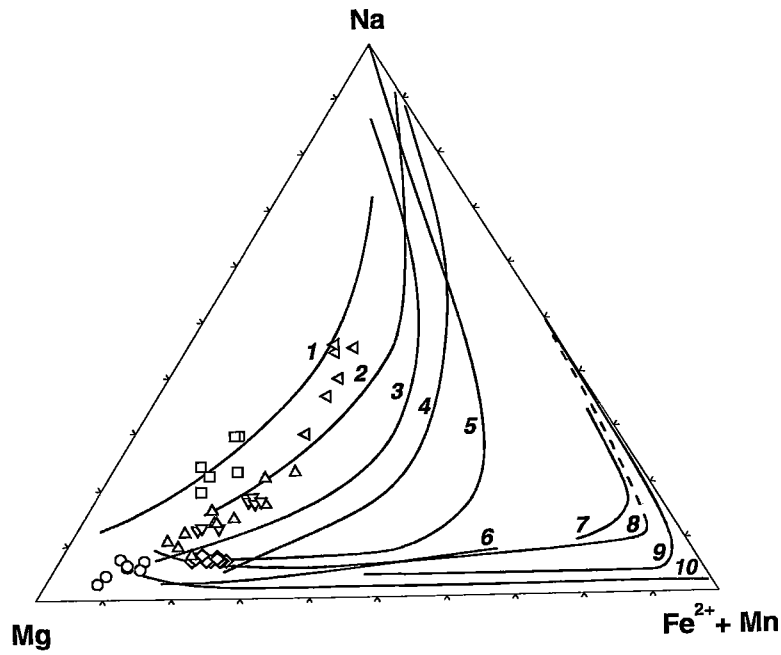

FIG. 5. Mg – Na – (Fe^{2+} + Mn) plot of the compositions of clinopyroxene in the Falcon Island pluton (in terms of atomic %). Symbols as in Figure 3. Numbered lines are trends from: undersaturated suites: (1) Auvergne, France (Varet 1969), (2) Itapirapuã, Brazil (Gomes *et al.* 1970), (3) Uganda (Tyler & King 1967), (4) Morotu, Japan (Yagi 1966), (5) Qôroq, Greenland (Stephenson 1972), (9) Ilímaussaq, Greenland (Larsen 1976), saturated to oversaturated suites: (6) Japanese alkali basalts (Aoki 1964), (7) pantellerite trend (Nicholls & Carmichael 1969), (8) Nandewar volcano, Australia (Abbott 1969), and (10) subalkaline pyroxenes from the silica-oversaturated Skaergaard intrusion, Greenland (Brown 1957, Brown & Vincent 1963).

inflection from iron enrichment to more sodic compositions can occur anywhere along the Fe^{2+}-enrichment trend and is a function of a complex interplay among oxygen fugacity, temperature, and the composition of the melt, most notably its increasing Na and decreasing Ca contents (Platt 1996). The degree of silica saturation and the agpaitic index of the magma also seem to play a role, as progressively later stages of Na enrichment are typical of agpaitic undersaturated, miaskitic undersaturated, peralkaline saturated, and metaluminous silica-saturated suites, respectively (Fig. 5) (Bonin & Giret 1985).

Crystallization of sodic pyroxenes is not exclusively indicative of high or increasing oxygen fugacities (Aoki 1964, Yagi 1966). Experiments have shown that aegirine is stable to conditions more reducing than those defined by the quartz – magnetite – fayalite (QFM) buffer (Bailey 1969). A sodium-enrichment trend is attributed to decreasing oxygen fugacity with fractionation at the Shonkin Sag laccolith (Nash & Wilkinson 1970), the Ilímaussaq intrusion (Larsen 1976), the Oslo rift (Neumann 1976), and the Coldwell complex (Mitchell & Platt 1978). The Falcon Island trend is similar to that of alkaline clinopyroxene from Shonkin Sag laccolith (Fig. 3), Uganda, Auvergne, Itapirapuã (Fig. 5), and the Oslo rift (Neumann 1976), but does not reach the aegirine end-member compositions of these other alkaline suites. The magma at Falcon Island did not achieve the peralkalinity required (*i.e.*, A.I. > 1) to form end-member aegirine (Neumann 1976, Bonin & Giret 1985). In this respect, the trend is similar to that in the Clériсy pluton, a Neoarchean ultrapotassic complex from the Abitibi Subprovince (Laflèche *et al.* 1991).

The Al content is sufficiently elevated in the clinopyroxene and the amphibole (see below) of all units of the pluton to fill the tetrahedral sites and to appear in the octahedral sites (Tables 2, 3). This feature is most probably a function of the composition of the magma, as the pluton is compositionally similar to

TABLE 3. CHEMICAL COMPOSITION OF AMPHIBOLE, FALCON ISLAND PLUTON

Sample #	182		32		33		31	
# of anal. / s.d.	6	s.d.	4	s.d.	3	s.d.	3	s.d.
SiO_2 (wt.%)	49.22	2.11	39.54	0.15	38.59	1.67	38.94	1.70
TiO_2	0.47	0.24	1.21	0.23	1.48	1.21	0.59	0.23
Al_2O_3	6.68	1.68	11.91	0.17	12.46	1.82	12.21	1.63
FeO	8.34	0.67	22.45	0.02	22.96	2.21	24.90	1.61
Cr_2O_3	0.16	0.06	0.01	0.01			0.02	0.02
MnO	0.18	0.05	0.56	0.05	0.59	0.02	0.65	0.02
MgO	17.67	0.73	7.60	0.19	6.48	0.92	5.76	1.22
CaO	12.2	0.41	10.55	0.03	9.33	0.40	8.75	0.12
Na_2O	2.04	0.42	2.69	0.01	3.33	0.30	3.72	0.20
K_2O	0.39	0.10	1.97	0.04	2.38	0.40	2.34	0.24
F	0.20	0.03	0.23	0.01	0.25	0.07	0.55	0.23
Cl	0.01		0.01					
Total	97.38	0.33	98.69	0.08	97.83	0.12	98.39	0.01
Structural formula based on 23 atoms of oxygen.								
TSi (a.p.f.u.)	7.03		6.05		6.00		6.05	
TAl	0.97		1.96		2.01		1.96	
CAl	0.15		0.19		0.27		0.26	
CCr	0.02							
CFe^{3+}	0.33		0.85		0.82		1.05	
CTi	0.05		0.14		0.17		0.07	
CMg	3.76		1.73		1.50		1.34	
CFe^{2+}	0.67		2.02		2.16		2.19	
CMn	0.02		0.08		0.08		0.09	
BCa	1.87		1.73		1.55		1.46	
BNa	0.13		0.28		0.45		0.55	
ANa	0.43		0.53		0.56		0.58	
AK	0.07		0.39		0.47		0.47	
Sum A	0.5		0.91		1.03		1.04	
Sum Cations	15.5		15.91		16.03		16.04	
CF	0.09		0.11		0.13		0.27	
Fe/(Mg+Fe)	0.21		0.62		0.67		0.71	
$Fe^{3+}/(Fe^{2+}+Fe^{3+})$	0.33		0.30		0.28		0.32	

Group-III ultrapotassic rocks, which are rich in Al and Ca (Foley *et al.* 1987). Other controls on the Al content of mafic minerals are temperature of crystallization, total pressure, oxygen fugacity and silica activity (Leake 1965, Helz 1973, Neumann 1976). Woolley *et al.* (1996) have documented high Al and Na contents in the clinopyroxene of some alkaline complexes, and attributed them to metamorphic re-equilibration. In metamorphosed clinopyroxene from these complexes, total Al is greater than 0.15 atoms per formula unit (*apfu*), whereas igneous clinopyroxene unaffected by metamorphism have Al less than 0.15 *apfu*, values similar to the clinopyroxene at Falcon Island (Table 2).

Amphibole

Amphibole occurs as subhedral to euhedral crystals mantling or interstitial to clinopyroxene. In melasyenite and syenite, the amphibole has a yellowish brown to dark green pleochroism and occurs as a mantle on clinopyroxene. In clinopyroxenite, the amphibole has a light yellow to medium green pleochroism and occurs as intergranular crystals and only rarely mantles clinopyroxene.

All units, with the exception of peraluminous alkali feldspar syenite, contain calcic amphibole. Average compositions (with standard deviations) are presented in Table 3, and the individual compositions are plotted on Figure 6 (based on the nomenclature of Leake *et al.* 1997). The amphibole in the clinopyroxenite ranges from edenite to magnesiohastingsite displaying decreasing Si (and correspondingly higher Al in the tetrahedral site) at relatively constant Fe and Mg contents, whereas amphibole from melasyenite and syenite range from magnesiohastingsite to hastingsite and show decreasing Mg at a relatively constant Si contents of 6 *apfu*. Average Fe/(Fe + Mg) values increase with fractionation (from about 0.2 in clinopyroxenite to about 0.7 in alkali feldspar syenite) (Table 3). Coincident increases in concentration of Mn, Na, K, and F, and decreases in Si and Ca are evident, but the amphibole suite does not achieve the degree of sodium enrichment evident in the clinopyroxene suite (Figs. 5, 7).

Mica

In alkaline volcanic rocks, leucite is commonly regarded as the indicator mineral of potassic character. However, in plutonic rocks, phlogopite, biotite and alkali feldspar are the diagnostic minerals (Luth 1967, Barton & Hamilton 1982, Corriveau & Gorton 1993). Mica is present in all units of the complex. In clinopyroxenite, it is a light yellow-green pleochroic phlogopite, which occurs as abundant medium-grained, anhedral poikilitic grains enclosing clinopyroxene grains. Dark green pleochroic biotite with a similar habit occurs in the monzodiorite, melasyenite, and syenite. Biotite is locally replaced by dark green chlorite in all units of the complex. Muscovite and biotite, without any accompanying pyroxene, amphibole or magnetite, occur in the peraluminous syenite. In this most fractionated unit, the biotite has a dark green pleochroism and occurs as fine-grained, subhedral plates. Muscovite is nonpleochroic and occurs as fine-grained, anhedral grains intergrown with biotite and feldspar.

Results of analyses of the mica are presented in Table 4. Structural formulas have been calculated on the basis of 24 atoms of oxygen. Wet-chemical determinations of FeO in biotite separated from the clinopyroxenite, monzodiorite and peraluminous alkali feldspar syenite was used in conjunction with electron-microprobe-determined FeO(total) to calculate Fe_2O_3, FeO, Fe^{2+} and Fe^{3+}. In the remaining samples, all iron was assumed to be Fe^{2+} in recalculation of the structural formulas.

No systematic intragrain zonation was observed. Biotite and phlogopite have octahedral-site occupancies ranging from 5.75 to 6.07 *apfu* (Table 4). Muscovite has a octahedral-site occupancy of 4.20 *apfu*. The Falcon Island suite displays a positive correlation of

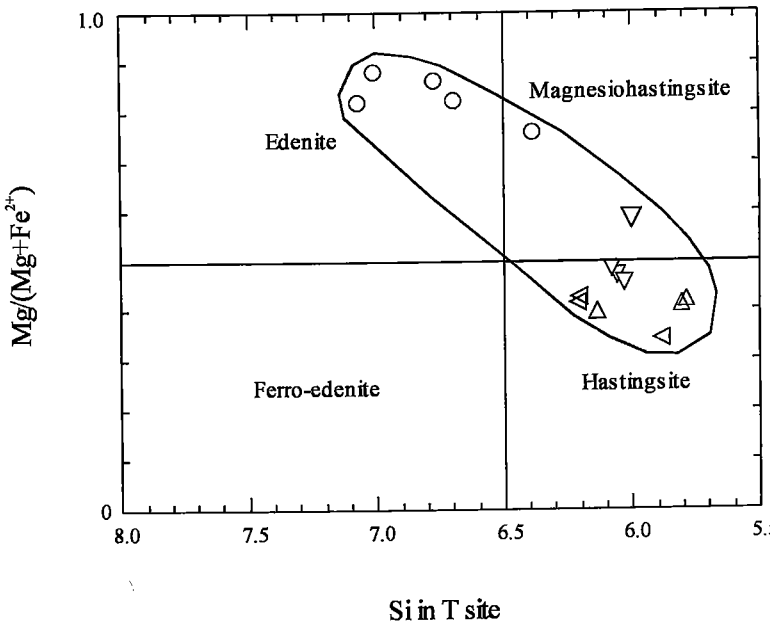

FIG. 6. Compositions of amphibole in the Falcon Island suite plotted on the calcic amphibole quadrilateral, for amphibole compositions with $Ca_B \geq 1.50$, $(Na + K)_A \geq 0.50$, $Ti < 0.50$, and $Fe^{3+} > {}^{VI}Al$ (Leake *et al.* 1997). Symbols as in Figure 3.

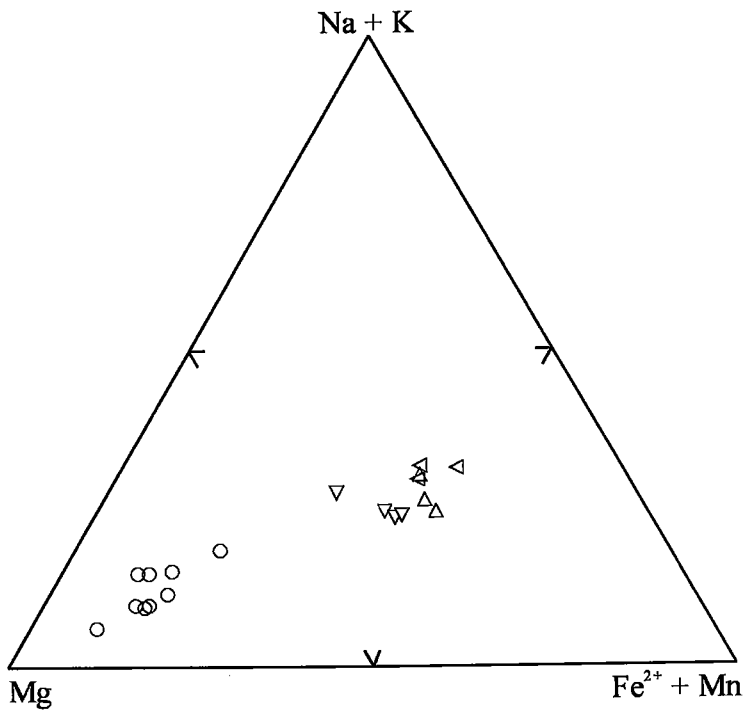

FIG. 7. Mg – (Na + K) – (Fe^{2+} + Mn) plot of the compositions of amphibole in the Falcon Island suite (in terms of atomic %). Symbols as in Figure 3.

TABLE 4. CHEMICAL COMPOSITION OF MICA, FALCON ISLAND PLUTON

sample #	182		185		33		32		31		190		261			
mineral	phlogopite		biotite		biotite		biotite		biotite		biotite		biotite		muscovite	
# of anal / s.d.	5	s.d	5	s.d	5	s.d	6	s.d	5	s.d	5	s.d	7	s.d	5	s.d
SiO_2 (wt%)	39.65	0.26	37.05	0.14	35.27	0.54	36.11	0.15	36.36	0.93	33.97	0.31	34.23	0.21	46.00	0.29
TiO_2	0.75	0.10	2.38	0.15	1.20	0.41	1.06	0.13	1.22	0.17	1.31	0.31	2.12	0.24	0.48	0.16
Al_2O_3	14.36	0.49	14.63	0.21	16.88	0.67	15.07	0.23	14.62	0.62	16.33	0.48	17.75	0.47	30.66	0.35
Cr_2O_3	0.16	0.03	0.02	0.02	0.02	0.02	0.01	0.01	0.01	0.01	0.00	0.00	0.01	0.01	0.01	0.01
FeO	5.83		14.21		22.01	1.33	20.78	0.54	23.32	1.52	22.72	0.32	21.09		5.88	0.29
Fe_2O_3	2.50		4.54										3.58			
MnO	0.11	0.02	0.27	0.03	0.54	0.07	0.47	0.06	0.57	0.04	0.60	0.04	0.47	0.03	0.04	0.01
MgO	21.62	0.42	13.29	0.19	10.20	0.70	12.40	0.44	9.87	1.19	9.44	0.19	7.50	0.31	1.39	0.17
CaO	0.00	0.00	0.00	0.01	0.01	0.02	0.02	0.01	0.06	0.06	0.01	0.01	0.01	0.01	0.01	0.01
Na_2O	0.21	0.03	0.10	0.02	0.08	0.03	0.05	0.01	0.07	0.01	0.08	0.01	0.08	0.03	0.18	0.03
K_2O	10.09	0.04	9.78	0.13	9.85	0.17	9.92	0.09	9.51	0.69	10.04	0.08	8.77	0.10	10.94	0.11
F	0.41	0.06	0.38	0.04	0.21	0.04	0.47	0.05	0.48	0.20	0.07	0.02	0.27	0.10	0.16	0.07
Cl	0.00	0.00	0.02	0.01	0.00	0.01	0.01	0.01	0.01	0.00	0.01	0.01	0.00	0.00	0.00	0.00
H_2O	1.80	0.03	1.70	0.02	1.76	0.02	1.64	0.03	1.61	0.09	1.83	0.01	1.73	0.05	4.31	0.03
Total	97.58		98.37		98.13		97.98		97.71		98.41		98.59		99.86	
O=F, Cl	0.21	0.03	0.16	0.02	0.09	0.02	0.20	0.02	0.20	0.09	0.01	0.01	0.11	0.04	0.07	0.03
Structural formula on the basis of 24 atoms of oxygen.																
TSi (a.p.f.u.)	5.74		5.65		5.46		5.59		5.70		5.25		5.31		6.29	
TAl	2.26		2.42		2.54		2.41		2.30		2.75		2.69		1.71	
CAl	0.19		0.17		0.54		0.34		0.40		0.77		0.60		3.22	
Ti	0.08		0.27		0.14		0.12		0.14		0.15		0.25		0.05	
Fe^{3+}	0.27		0.51										0.42			
Fe^{2+}	0.72		1.79		2.85		2.69		3.06		2.94		2.73		0.66	
Cr	0.02		0.00		0.00		0.00		0.00		0.00		0.00		0.00	
Mn	0.01		0.03		0.07		0.06		0.08		0.08		0.06		0.00	
Mg	4.67		2.98		2.35		2.86		2.31		1.94		1.73		0.28	
total octahedral	5.86		5.75		5.95		6.07		5.99		5.88		5.69		4.20	
Ca	0.00		0.00		0.00		0.00		0.01		0.00		0.00		0.00	
Na	0.06		0.03		0.02		0.02		0.02		0.02		0.02		0.05	
K	1.86		1.88		1.96		1.96		1.80		1.98		1.93		1.91	
Cations	15.89		15.68		15.94		16.05		15.92		16.89		15.70		14.16	
F	0.38		0.36		0.21		0.46		0.48		0.07		0.26		0.14	
Cl	0.00		0.01		0.00		0.01		0.00		0.00		0.01		0.00	
OH	1.74		1.74		1.82		1.70		1.68		1.89		1.79		3.93	
O	24.00		24.00		24.00		24.00		24.00		24.00		24.00		24.00	
Fe/(Fe+Mg)	0.17		0.44		0.56		0.48		0.57		0.60		0.65		0.70	
$Fe^{3+}/(Fe^{2+}+Fe^{3+})$	0.27		0.22										0.13			

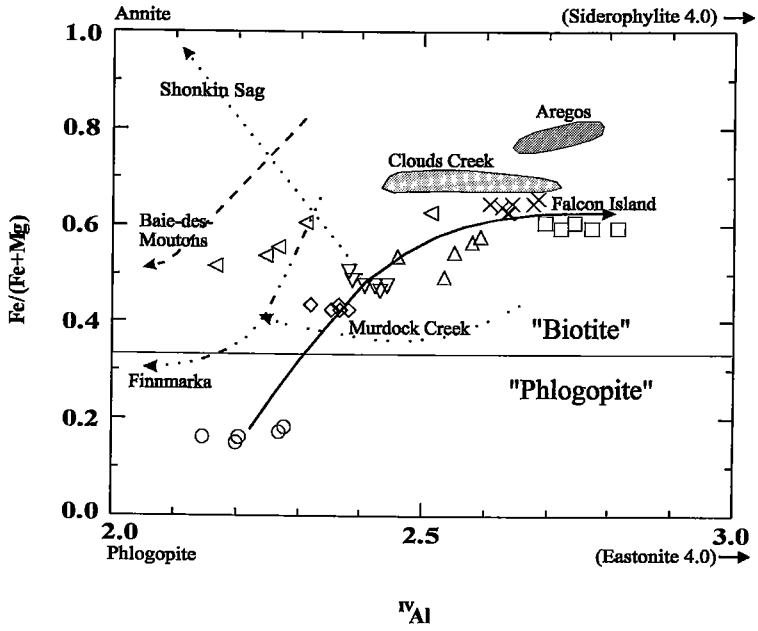

FIG. 8. Biotite compositions from the Falcon Island pluton plotted on part of the phlogopite – annite – eastonite – siderophyllite quadrilateral. The crystallization paths (arrows) of biotite from other differentiated alkaline complexes including Finnmarka (Czamanske & Wones 1973), Baie-des-Moutons (Lalonde & Martin 1983), Shonkin Sag (Nash & Wilkinson 1970) and Murdock Creek (Rowins *et al.* 1991) also are shown for comparison. Fields of biotite from S-type granites from Aregos (de Albuquerque 1973) and Clouds Creek (Speer 1984) plutons also are shown. Symbols as in Figure 3. The "x" symbols represents biotite from the peraluminous alkali feldspar syenite, sample 88–261.

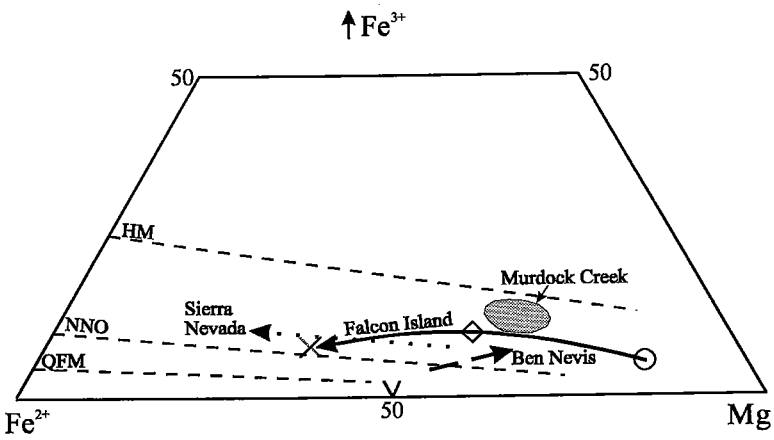

FIG. 9. Fe^{3+} – Fe^{2+} – Mg contents of biotite from the Falcon Island suite. Dashed lines represent compositions of "buffered" biotite , Hematite – Magnetite (HM), Nickel – Nickel Oxide (NNO) and Quartz – Fayalite – Magnetite (QFM) in the system annite – phlogopite – $KFe^{3+}{}_3AlSi_3O_{12}(H_{-1})$ (Wones & Eugster 1965). Paths of crystallization for biotite from other felsic plutons, including the Sierra Nevada batholith (Dodge *et al.* 1969), Ben Nevis (Haslam 1968) and Murdock Creek (Rowins *et al.* 1991), also are shown for comparison. Symbols as in Figure 9.

enrichment in Fe/(Fe + Mg) and ^{IV}Al with fractionation (Fig. 8). The only other alkaline suite displayed on Figure 8 that has increasing Fe/(Fe + Mg) with fractionation is the Shonkin Sag laccolith, which Nash & Wilkinson (1970) attributed to reduction. Other alkaline complexes, such as the Finnmarka (Czamanske & Wones 1973), Ben Nevis (Haslam 1968), Baie-des-Moutons (Lalonde & Martin 1983), and Murdock Creek (Rowins *et al.* 1991), have decreasing or flat Fe/(Fe + Mg) trends attributed to increasing or constant $f(O_2)$ with fractionation. A progressive increase in the ^{IV}Al content of biotite with fractionation is only evident in the Falcon Island suite. In fact, the trend to a biotite–muscovite, peraluminous, quartz-saturated, syenite end-member [sample #88–261; Aluminum Saturation Index (ASI) = 1.1, normative quartz = 0.8%; Table 1] is somewhat unusual in alkaline igneous systems. Biotite from all but one of the syenite samples (sample #93–31) have elevated ^{IV}Al contents and Fe/(Fe + Mg) values similar to those of peraluminous granites (Fig. 8) (De Albuquerque 1973, Speer 1984).

Variation in ^{IV}Al content in biotite may be controlled by variables such as silica activity, temperature, and total pressure (Czamanske & Wones 1973, Thompson 1974). As both the Shonkin Sag laccolith and the Falcon Island complex are interpreted to have evolved from reducing magmatic systems, differences in the ^{IV}Al trends of the biotite in the two intrusions may be the result of different total pressure. The Shonkin Sag laccolith was emplaced at a very shallow depth, with an estimated total pressure of 0.3 kbar (Nash & Wilkinson 1970). The Falcon Island complex is constrained between a minimum of about 3.5 kbar for igneous muscovite (Speer 1984) and a maximum of about 4 kbar defined by regional metamorphic assemblages in metasedimentary enclaves and country-rock units that contain andalusite, staurolite and almandine (Ayer 1991).

Another factor controlling Al content may be the precipitation of hornblende and clinopyroxene, both of which have relatively low ASI values and can drive a subaluminous magmatic system to produce mildly peraluminous late fractionates (Zen 1986). Contamination by sedimentary rocks, which form in the surrounding country-rocks and occur as a large enclave in the southwestern end of the pluton (Fig. 2), could also be responsible for Al enrichment. Silica-saturated end-members have been attributed to assimilation of sedimentary rocks in a number of alkaline complexes (Fowler 1988, Laflèche *et al.* 1991, Landoll & Foland 1996). On-going isotopic studies on the pluton may help to clarify the process of enrichment.

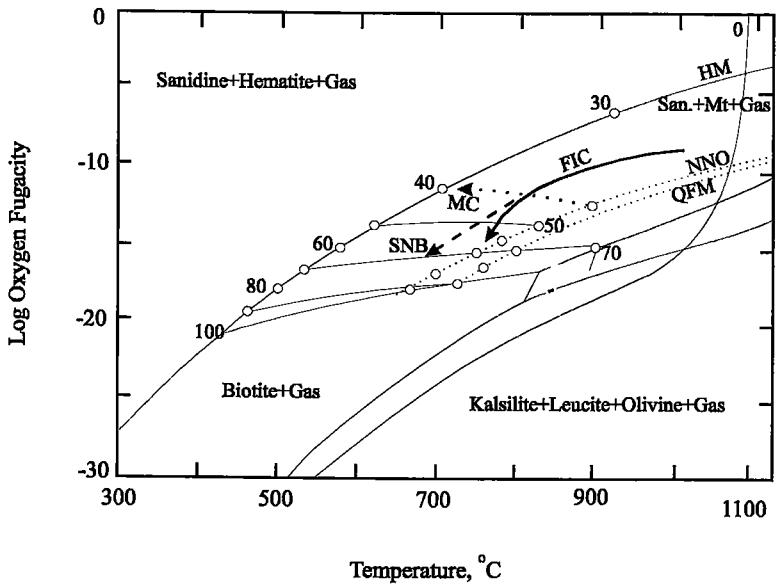

FIG. 10. Stability of biotite with differing Fe/(Fe+Mg) ratios as a function of oxygen fugacity and temperature at 2070 bars total pressure (Wones & Eugster 1965). Numbers (30–100) represent the 100Fe/(Fe+Mg) values of biotite in the assemblage biotite + alkali feldspar + magnetite on the same buffer curves as in Figure 10. Crystallization paths for the Falcon Island complex (FIC), Murdock Creek pluton (MC) (Rowins *et al.* 1991) and the Sierra Nevada batholith (SNB) (Dodge *et al.* 1969) are shown for comparison.

The Ti content of the biotite at Falcon Island is relatively low and increases from 0.09 to 0.26 *apfu* with fractionation. This trend may also be caused by progressive reduction with fractionation. Oxidized alkaline complexes such as Murdock Creek typically display decreasing Ti content with fractionation (Rowins *et al.* 1991). The Mn content in biotite also increases with fractionation from 0.02 to 0.09 *apfu*. A trend of increasing Mn is observed in both oxidized complexes such as Finnmarka (Czamanske & Wones 1973), Klokken (Parsons 1979) and Murdock Creek (Rowins *et al.* 1991) and in reduced plutons, such as the Sierra Nevada batholith (Ague & Brimhall 1988).

Reduction is indicated by a decline in the $Fe^{3+}/(Fe^{2+} + Fe^{3+})$ values of biotite, determined by wet-chemical analyses of biotite separates. The values decline from 0.27 in clinopyroxenite, to 0.22 in monzodiorite, to 0.13 in the peraluminous syenite (Table 4). Wones & Eugster (1965) have provided estimates of the compositions of biotite coexisting with alkali feldspar and magnetite under various oxygen-buffered conditions. The atomic proportions of Fe^{2+}:Fe^{3+}:Mg for three biotite separates are shown in Figure 9. They plot as a broad trend of increasing Fe^{2+} and decreasing Mg with fractionation within the field bounded by the nickel – nickel oxide (NNO) and hematite – magnetite (HM) buffers. Compared to other plutonic suites, the Falcon Island trend is parallel to the reducing trend of the calc-alkaline Sierra Nevada batholith (Dodge *et al.* 1969), and is opposite to that of oxidized alkaline plutonic suites such as the Ben Nevis (Haslam 1968) and Murdock Creek (Rowins *et al.* 1991) complexes.

Wones & Eugster (1965) related the atomic ratio 100Fe/(Fe + Mg) during biotite crystallization to temperature and $f(O_2)$ (Fig. 10). The precise location of the fractionation path for the Falcon Island suite is uncertain, but the relative position is constrained by several factors: (1) 100Fe/(Fe + Mg) values in biotite ranging from 17 to 65 (Table 4, Fig. 8), (2) the field constrained by the HM and the NNO buffers (Fig. 9), and (3) a trend that is progressively closer to the NNO buffer in the more fractionated rocks (Fig. 9), *i.e.*, declining relative $f(O_2)$. Collectively, these features indicate decreasing $f(O_2)$ from about 10^{-10} to 10^{-15} in conjunction with a decline in temperatures from about 1000° to 750°C and a declining relative $f(O_2)$ with fractionation. Declining relative $f(O_2)$ is a more precise indicator of reducing magmatic conditions (Frost 1991, Frost & Lindsley 1991). This extensive range from oxidized cumulates to highly reduced fractionates is

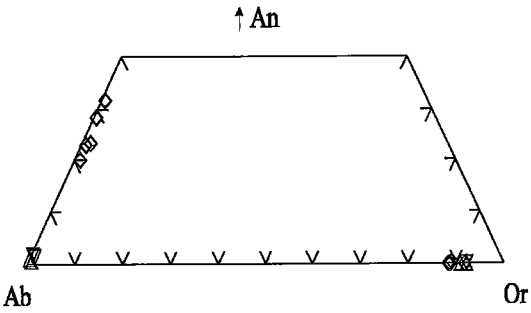

FIG. 11. Compositions of the feldspar in the Falcon Island pluton in terms of end-member compositions for albite (Ab), orthoclase (Or) and anorthite (An) (Deer *et al.* 1963b). Symbols as in Figure 3.

clearly different from the oxidation trend of the Murdock Creek suite (Rowins *et al.* 1991), and is similar in trend to the trend for the Sierra Nevada batholith (Dodge *et al.* 1969) (Fig. 10). Increasing the total pressure from about 2 kbar (the pressure utilized in the experiments for construction of Fig. 10) to a total pressure of 4 kbar (the estimated emplacement pressure of the pluton) would shift biotite isopleths to slightly higher temperatures, but would have little effect on $f(O_2)$ (Wones & Eugster 1965).

Feldspars and nepheline

Coarse-grained subhedral alkali feldspar occurs as phenocrysts in monzodiorite, alkali feldspar melasyenite, and alkali feldspar syenite. These grains typically have a perthitic core with finely exsolved albite, and a nonperthitic rim. Plagioclase and microcline form as small distinct anhedral crystals intergranular to the phenocrysts. The sequence of early perthitic alkali feldspar followed by coexisting alkali feldspar and plagioclase suggests a change from hypersolvus to subsolvus conditions of crystallization and thus increasing $P(H_2O)$ with fractionation (Tuttle & Bowen 1958, Martin & Bonin 1976). Increasing $P(H_2O)$ is also independently supported by an evolution from early-crystallized clinopyroxene to later hydrous phases such as amphibole and biotite.

The plagioclase in syenites is albite ($An_{0.75}$ to $An_{1.6}$), whereas in monzodiorite it is normally zoned and ranges from An_{32} to An_{20} (Fig. 11). Alkali feldspar from melasyenite and monzodiorite show small decreases in K content (from Or_{92} to Or_{89}), decrease in Sr, from 0.60% to 0.33% SrO, and a substantial increase in Ba, from 0.42% to 2.79% BaO. Alkali feldspar from the monzodiorite lacks the distinctive tartan twinning evident in the microcline of more fractionated units and may be a higher-temperature, more disordered variety. Barium-rich feldspar and localized inclusions of barite in the cores of large crystals of diopside indicate that the early mafic cumulates were derived from a barium- and SO_4-enriched magma.

The nepheline occurs as fine-grained anhedral crystals interstitial to microcline and albite in syenite and melasyenite. The nepheline is a relatively Ca-poor and K-rich variety similar to that documented from other nepheline syenites (Deer *et al.* 1963b).

Fe–Ti oxides

Magnetite is common in all but the most fractionated rocks of the complex. The early mafic units contain abundant magnetite and a minor amount of subhedral ilmenite crystals commonly intergrown with magnetite. Magnetite may display variable degrees of alteration to hematite, preferentially developed along the margin of grains, oriented partings and irregular fractures. In many cases, the grains of magnetite also have a rim of "leucoxene" or titanite, which is interpreted to be the result of subsolidus oxidation (Carmichael & Nicholls 1967).

Only the clinopyroxenite has elevated Cr in whole-rock analyses (1200 ppm Cr; Table 1). The magnetite of clinopyroxenite contains an average of 2.35% Cr_2O_3. The other units of the pluton are relatively Cr-poor (161 to 7 ppm Cr), as is their magnetite. For example, the magnetite in monzodiorite has an average of 0.27% Cr_2O_3. The mafic silicate minerals of all units are also relatively depleted in Cr, including those of the clinopyroxenite (Tables 2, 3, 4). The above features indicate that most of the Cr content of the magma was concentrated in magnetite, and depleted early in the fractionation sequence. Some of the the larger crystals of diopside in monzodiorite exhibit concentric bands containing abundant tiny acicular inclusions of oxide oriented at right angles. Although too small for accurate electron-microprobe analysis, the elevated Fe and Cr contents of these inclusions suggest they are a Cr-rich iron oxide. Similar-appearing inclusions in clinopyroxene in the Murdock Creek complex were identified as Cr-rich magnetite (Rowins *et al.* 1991).

Although the ferrous/ferric ratio of minerals has long been used as a monitor of oxygen fugacity, a better measure of oxidation or reduction is the relative $f(O_2)$, a measure of $f(O_2)$ minus the QFM buffer values (Ghiorso & Sack 1991). This value is commonly determined from the compositions of the Fe–Ti oxide minerals in a rock. At Falcon Island, magnetite and minor ilmenite were the only oxides to crystallize from the magma. The nearly pure end-member compositions of magnetite and ilmenite, the very low Ti content of the magnetite, and the occurrence of a rim of "leucoxene" and titanite around the magnetite crystals suggest subsolidus re-equilibration from an originally more titaniferous composition. Low-temperature re-equilibration of the oxides precludes their utilization as petrogenetic indicators of the magma's evolution

(Frost & Lindsley 1991). The current end-member compositions, <5 mol.% ulvöspinel content in magnetite and >98% mol.% ilmenite, suggest that the re-equilibration temperatures were less than 500°C (Ghiorso & Sack 1991, p. 261) and probably related to postmagmatic hydrothermal fluids in a late metamorphic or alteration event.

Discussion and Conclusions

The Falcon Island complex is an Archean, undersaturated, ultrapotassic pluton. Ayer & Davis (1997) speculated that the complex and coeval shoshonitic volcanic rocks of the Electrum Lake Assemblage in the northern part of the Lake of the Woods greenstone belt may have been derived from a mantle-wedge source beneath a Neoarchean mature island arc or a continental arc source. This hypothesis was based on chemical characteristics such as highly fractionated rare-earth element (*REE*) patterns, enrichment in large-ion lithophile elements, and depletion in high field-strength elements (*HFSE*) similar to those of modern arc suites. Low-degree partial melts of mantle material beneath island arcs tend to have high contents of alkalis and *REE*, low *HFSE* and high oxygen fugacities (Foley & Wheller 1990).

The Falcon Island magma evolved with increasing $P(H_2O)$, as indicated by the transition from early crystallization of clinopyroxene to amphibole and biotite, and from an early hypersolvus texture to a later subsolvus assemblage. An "aegirine-enrichment trend" is evident in the clinopyroxene as progressive depletion in Mg and Ca, and enrichment in Fe and Na, both as zoning in individual grains and in the successively fractionated units (Figs. 3–5). Mg-rich diopside in clinopyroxenite was followed by edenite and phlogopite. In monzodiorite, diopside was followed by biotite and normally zoned plagioclase (An_{32} to An_{20}). In alkali feldspar melasyenite and alkali feldspar syenite, Fe-rich diopside cores evolved to aegirine augite and hastingsite rims and was followed by albite ($An_{1.6}$ to $An_{0.7}$).

Elevated Al is evident in whole-rock compositions and is reflected in the Al content of clinopyroxene, amphibole and biotite, characteristics that are typical of the Group-III ultrapotassic suites from modern collisional orogenic areas (Foley *et al.* 1987). On the basis of its mineral assemblages, and those of metasedimentary enclaves, the Falcon Island pluton was emplaced at a mid-crust level. The relatively elevated ^{VI}Al-content of the clinopyroxene is similar to that of the alkaline Murdock Creek pluton in the Kirkland Lake camp of the Abitibi Subprovince, emplaced at a similar depth in the crust (Rowins *et al.* 1991). However, differences in Al evolution with fractionation are evident in the biotite trends of the two intrusions. Biotite at Murdock Creek shows a depletion in ^{IV}Al at constant Fe/(Fe + Mg), whereas at Falcon Island, the biotite displays increasing ^{IV}Al and Fe/(Fe + Mg) with fractionation. The differing trends are probably the result of a variety of factors including: differing $f(O_2)$ paths, differing relative ASI values, the types and relative abundance of precipitating minerals, and a differing type of crustal contaminant.

The lack of olivine (or olivine pseudomorphs) in all rocks and the presence of titanite, magnetite and diopside in the early-crystallized mafic units indicate crystallization under more oxidizing conditions than those defined by the QFM buffer (Carmichael & Nicholls 1967, Neumann 1976). During ascent and cooling, magmas tend to follow temperature – $f(O_2)$ paths parallel to major buffers. Loss of oxidized or reduced, solid or gaseous species produces deviations from this path. Formation of minerals with a higher proportion of Fe^{3+} than are present in the melt, such as magnetite, causes reduction.

The redox conditions of alkaline complexes may have economic significance. Late Archean alkali-rich intrusive rocks have been implicated in models of gold mineralization on the basis of their close spatial and temporal association (Rock & Groves 1988, Wyman & Kerrich 1989, Sutcliffe *et al.* 1990, Robert 1997). Fyon *et al.* (1989) suggested that gold mineralization and alkaline magmatism may be a manifestation of the cratonization process involving mantle-derived melts and CO_2. Cameron & Hattori (1987) have proposed that gold mineralization in the Kirkland Lake camp originates from oxidized hydrothermal fluids derived from magmatic sources. Many of the syenites associated with mineralization in the Kirkland Lake gold camp represent oxidized magmas with possible links to the gold-bearing fluids (Cameron & Carrigan 1987, Rowins *et al.* 1991, Lévesque 1994).

Environments of gold mineralization in the Lake of the Woods greenstone belt have both porphyry and shear-zone associations (Davis & Smith 1991). There is, however, no evidence of anomalous gold mineralization in the vicinity of the Falcon Island pluton, despite its alkaline nature and the proximity of potentially favorable shear-zones (Ayer 1991). This fact suggests a negative correlation between gold mineralization and reduced alkaline plutons. The Falcon Island complex is comparable in its array of rock types and depth of emplacement to syenitic complexes associated with gold mineralization in the Kirkland Lake camp, but there are significant differences in the redox state of the evolving magmas. It would therefore appear that alkaline complexes associated with progressively reduced magmatic fluids, such as the Falcon Island complex, have less potential to produce the oxidized hydrothermal fluids conducive to gold mineralization. Thus analyzing the composition of ferromagnesian minerals in a differentiated complex, and in particular the biotite, may provide an additional tool with which to evaluate their potential to produce gold deposits.

ACKNOWLEDGEMENTS

This paper is published with the permission of the Senior Manager of the Precambrian Geoscience Section, Ontario Geological Survey, Ministry of Northern Development and Mines.

Field work was supported by the Ontario Geological Survey. Dave Crabtree is thanked for his assistance with the electron-microprobe work at the Geoscience Laboratories, Ontario Geoservices Centre, Sudbury, Ontario. I thank André Lalonde for many stimulating discussions on the applications of mineral chemistry, which have in part inspired this research. Reviews by Bernard Bonin, Louise Corriveau, Tony Fowler, Robert Martin, Denver Stone and Phil Thurston have helped to improve the manuscript.

REFERENCES

ABBOTT, M.J. (1969): Petrology of the Nandewar volcano, N.S.W. Australia. *Contrib. Mineral. Petrol.* **20**, 115-134.

AGUE, J.J. & BRIMHALL, G.H. (1988): Regional variations in bulk chemistry, mineralogy and the compositions of mafic and accessory minerals in the batholiths of California. *Geol. Soc. Am., Bull.* **100**, 891-911.

AOKI, K.-I. (1964): Clinopyroxenes from alkaline rocks of Japan. *Am. Mineral.* **49**, 1199-1223.

AYER, J.A. (1991): Geology of the Falcon Island area, Lake of the Woods, District of Kenora. *Ont. Geol. Surv., Open File Rep.* **5804**.

_____ & BUCK, S. (1989): Geology of the Chisholm Island area, Lake of the Woods, District of Kenora. *Ont. Geol. Surv., Open File Rep.* **5710**.

_____ & DAVIS, D.W. (1997): Neoarchean evolution of differing convergent margin assemblages in the Wabigoon Subprovince: geochemical and geochronological evidence from the Lake of the Woods greenstone belt, Superior Province, northwestern Ontario. *Precambrian Res.* **81**, 155-178.

BAILEY, D.K. (1969): The stability of acmite in the presence of H_2O. *Am. J. Sci.* **267-A**, 1-16.

BARTON, M. & HAMILTON, D.L. (1982): Water-undersaturated melting experiments bearing upon the origin of potassium-rich magmas. *Mineral. Mag.* **45**, 267-278.

BEN OTHMAN, D., ARNDT, N.T., WHITE, W.M. & JOCHUM, K.P. (1990): Geochemistry and age of Timiskaming alkali volcanics and the Otto syenite stock, Abitibi, Ontario. *Can. J. Earth Sci.* **27**, 1304-1311.

BLICHERT-TOFT, J., ARNDT, N.T. & LUDDEN, J.N. (1996): Precambrian alkaline magmatism. *Lithos* **37**, 97-111.

BONIN, B. & GIRET, A. (1985): Clinopyroxene compositional trends in oversaturated and undersaturated alkaline ring complexes. *J. Afr. Earth Sci.* **3**, 175-183.

BROWN, G.M. (1957): Pyroxenes from the early and middle stages of fractionation of the Skaergaard intrusion, East Greenland. *Mineral. Mag.* **31**, 511-543.

_____ & VINCENT, E.A. (1963): Pyroxenes from the late stages of fractionation of the Skaergaard intrusion, East Greenland. *J. Petrol.* **4**, 175-197.

CAMERON, E.M. & CARRIGAN, W.J. (1987): Oxygen fugacity of Archean felsic magmas: relationship to gold mineralization. *Geol. Sur. Can. Pap.* **87-1A**, 281-298.

_____ & HATTORI, K. (1987): Archean gold mineralization and oxidized hydrothermal fluids. *Econ. Geol.* **82**, 1177-1191.

CARMICHAEL, I.S.E. & NICHOLLS, J. (1967): Iron–titanium oxides and oxygen fugacities in volcanic rocks. *J. Geophys. Res.* **72**, 4665-4687.

CAWTHORN, R.G. & COLLERSON, K.D. (1974): The recalculation of pyroxene end-member parameters and the estimation of ferrous and ferric iron content from electron microprobe analyses. *Am. Mineral.* **59**, 1203-1208.

CORRIVEAU, L. & GORTON, M.P. (1993): Coexisting K-rich alkaline and shoshonite magmatism of arc affinities in the Proterozoic: a reassessment of syenitic stocks in the southwestern Grenville Province. *Contrib. Mineral. Petrol.* **113**, 262-279.

CZAMANSKE, G.K. & WONES, D.R. (1973): Oxidation during magmatic differentiation, Finnmarka complex, Oslo area, Norway. II. The mafic silicates. *J. Petrol.* **14**, 349-380.

DAVIS, D.W., BLACKBURN, C.E. & KROGH, T.E. (1982): Zircon U–Pb ages from the Wabigoon – Manitou lakes region, Wabigoon Subprovince, northwest Ontario. *Can. J. Earth Sci.* **19**, 254-266.

_____ & SMITH, P.M. (1991): Archean gold mineralization in the Wabigoon Subprovince, a product of crustal accretion: evidence from U–Pb geochronology in the Lake of the Woods area, Superior Province, Canada. *J. Geol.* **99**, 337-353.

DE ALBUQUERQUE, C.A.R. (1973): Geochemistry of biotites from granitic rocks, northern Portugal. *Geochim. Cosmochim. Acta* **37**, 1779-1802.

DEER, W.A., HOWIE, R.A. & ZUSSMAN, J. (1963a): *Rock-Forming Minerals.* **3.** *Sheet Silicates.* Longman, London, U.K.

_____, _____ & _____ (1963b): *Rock-Forming Minerals.* **4.** *Framework Silicates.* Longman, London, U.K.

DODGE, F.C.W., SMITH, V.C. & MAYS, R.E. (1969): Biotites from granitic rocks of the central Sierra Nevada batholith, California. *J. Petrol.* **10**, 250-271.

FOLEY, S.F., VENTURELLI, D.H., GREEN, D.H. & TOSCANI, L. (1987): The ultrapotassic rocks: characteristics,

classification, and constraints for petrogenetic models. *Earth Sci. Rev.* **24**, 81-134.

_____ & WHELLER, G.E. (1990): Parallels in the origin of the geochemical signatures of island arc volcanics and continental potassic igneous rocks: the role of residual titanites. *Chem. Geol.* **85**, 1-18.

FOWLER, M.B. (1988): Elemental evidence for crustal contamination of mantle-derived Caledonian syenite by metasedimentary anatexis and magma mixing. *Chem. Geol.* **69**, 1-16.

FROST, B.R. (1991): Introduction to oxygen fugacity. *In* Oxide Minerals: Petrologic and Magnetic Significance (D.H. Lindsley, ed.). *Rev. Mineral.* **25**, 1-9.

_____ & LINDSLEY, D.H. (1991): Occurrence of iron–titanium oxides in igneous rocks. *In* Oxide Minerals: Petrologic and Magnetic Significance (D.H. Lindsley, ed.). *Rev. Mineral.* **25**, 433-468.

FYON, J.A., TROOP, D.G., MARMONT, S. & MACDONALD, A.J. (1989): Introduction of gold into Archean crust, Superior Province, Ontario: coupling between mantle initiated magmatism and lower crustal thermal maturation. *Econ. Geol., Monogr.* **6**, 479-490.

GHIORSO, M.S. & SACK, R.O. (1991): Thermochemistry of the oxide minerals. *In* Oxide Minerals: Petrologic and Magnetic Significance (D.H. Lindsley, ed.). *Rev. Mineral.* **25**, 221-264.

GIBB, F.G.F. (1973): The zoned clinopyroxene of the Shiant Isles sill, Scotland. *J. Petrol.* **14**, 203-230.

GOMES, C.B., MORO, S.L. & DUTRA, C.V. (1970): Pyroxenes from the alkaline rocks of Itapirapuã, San Paulo, Brazil. *Am. Mineral.* **55**, 224-230.

HASLAM, H.W. (1968): The crystallization of intermediate and acid magmas at Ben Nevis, Scotland. *J. Petrol.* **9**, 84-104.

HELZ, R.T. (1973): Phase relations of basalts in their melting range at $P(H_2O)$ = 5 kbars as a function of oxygen fugacity. *J. Petrol.* **14**, 249-302.

LAFLÈCHE, M.R., DUPUY, C. & DOSTAL, J. (1991): Archean orogenic ultrapotassic magmatism: an example from the southern Abitibi greenstone belt. *Precamb. Res.* **52**, 71-96.

LALONDE, A.E. & MARTIN, R.F. (1983): The Baie-des-Moutons syenitic complex, La Tabatière, Quebec. II. The ferromagnesian minerals. *Can. Mineral.* **21**, 81-91.

LANDOLL, J.D. & FOLAND, K.A. (1996): The formation of quartz syenite by crustal contamination at Mont Shefford and other Monteregian complexes, Quebec. *Can. Mineral.* **34**, 301-324.

LARSEN, L.M. (1976): Clinopyroxene and coexisting mafic minerals from the alkaline Ilímaussaq intrusion, South Greenland. *J. Petrol.* **17**, 258-290.

LEAKE, B.E. (1965): The relationship between tetrahedral aluminium and the maximum possible octahedral aluminium in natural calciferous and subcalciferous amphiboles. *Am. Mineral.* **50**, 843-851.

_____ and 21 others (1997): Nomenclature of amphiboles: report of the Subcommittee on Amphiboles of the International Mineralogical Association, Commission on New Minerals and Mineral Names. *Can. Mineral.* **35**, 219-246.

LE BAS, M.J. (1962): The role of aluminium in igneous clinopyroxenes with relation to their parentage. *Am. J. Sci.* **260**, 267-288.

LÉVESQUE, G. (1994): *Duality of Magmatism at Kirkland Lake, Ontario, Canada.* M.Sc. thesis, Univ. Ottawa, Ottawa, Ontario.

LUTH, W.C. (1967): Studies in the system $KAlSiO_4$–Mg_2SiO_4–SiO_2–H_2O. I. inferred phase relations and petrologic applications. *J. Petrol.* **8**, 372-416.

MARTIN, R.F. & BONIN, B. (1976): Water and magma genesis: the association hypersolvus granite – subsolvus granite. *Can. Mineral.* **14**, 228-237.

MCGUIRE, A.V., DYAR, M.D. & WARD, K.A. (1989): Neglected Fe^{3+}/Fe^{2+} ratios – a study of Fe^{3+} content of megacrysts from alkali basalts. *Geology* **17**, 687-690.

MCNEIL, A.M. & KERRICH, R. (1986): Archean lamprophyre dykes and gold mineralization, Matheson, Ontario: the conjunction of LILE-enriched mafic magmas, deep crustal structures and Au concentration. *Can. J. Earth Sci.* **23**, 324-343.

MITCHELL, R.H. (1996): Classification of undersaturated and related alkaline rocks. *In* Undersaturated Alkaline Rocks: Mineralogy, Petrogenesis, and Economic Potential (R.H. Mitchell, ed.). *Mineral. Assoc. Can., Short-Course Handbook* **24**, 1-22.

_____ & PLATT, R.G. (1978): Mafic mineralogy of ferroaugite syenite from the Coldwell alkalic complex, Ontario, Canada. *J. Petrol.* **19**, 627-651.

MORIMOTO, N. (1989): Nomenclature of pyroxenes. *Can. Mineral.* **27**, 143-156.

NASH, W.P. & WILKINSON, J.F.G. (1970): Shonkin Sag laccolith, Montana. 1. Mafic minerals and estimates of temperature, pressure, oxygen fugacity and silica activity. *Contrib. Mineral. Petrol.* **25**, 241-269.

NEUMANN, E.-R. (1976): Compositional relations among pyroxenes, amphiboles and other mafic phases in the Oslo region plutonic rocks. *Lithos* **9**, 85-109.

NICHOLLS, J. & CARMICHAEL, I.S.E. (1969): Peralkaline acid liquids: a petrological study. *Contrib. Mineral. Petrol.* **20**, 268-294.

PARSONS, I. (1979): The Klokken gabbro–syenite complex, South Greenland: cryptic variation and origin of inversely graded layering. *J. Petrol.* **20**, 653-694.

PLATT, G.R. (1996): Nepheline syenite complexes – an overview. *In* Undersaturated Alkaline Rocks: Mineralogy, Petrogenesis, and Economic Potential (R.H. Mitchell, ed.). *Mineral. Assoc. Can., Short-Course Handbook* **24**, 63-99.

ROBERT, F. (1997): A preliminary geological model for syenite-associated disseminated gold deposits in the Abitibi belt, Ontario and Quebec. *Geol. Surv. Can., Current Res.* **1997-C**, 201-210.

ROBINSON, P., SPEAR, F.S., SCHUMACHER, J.C., LAIRD, J., KLEIN, C., EVANS, B.W. & DOOLAN, B.L. (1982): Phase relations of metamorphic amphiboles: natural occurrence and theory. *In* Amphiboles: Petrology and Experimental Phase Relations (D.R. Veblen & P.H. Ribbe, eds.). *Rev. Mineral.* **9B**, 1-227.

ROCK, N.M.S. & GROVES, D.I. (1988): Can lamprophyres resolve the genetic controversy over mesothermal gold deposits? *Geology* **16**, 538-541.

ROWINS, S.M., CAMERON, E.I., LALONDE, A.E. & ERNST, R.E. (1993): Petrogenesis of the late Archean syenitic Murdock Creek pluton, Kirkland Lake, Ontario: evidence for an extensional tectonic setting. *Can. Mineral.* **31**, 219-244.

_____, LALONDE, A.E. & CAMERON, E.M.I. (1991): Magmatic oxidation in the syenitic Murdock Creek intrusion, Kirkland Lake, Ontario: evidence from the ferromagnesian silicates. *J. Geol.* **99**, 395-414.

SINCLAIR, W.A. (1982): Gold deposits of the Matachewan area, Ontario. *Can. Inst. Mining Metall., Spec. Vol.* **24**, 83-93.

SØRENSEN, H. (1974): Alkali syenites, feldspathoidal syenites and related lavas. *In* The Alkaline Rocks (H. Sørensen, ed.). John Wiley & Sons, New York, N.Y. (22-52).

SPEER, J.A. (1984): Micas in igneous rocks. *In* Micas (S.W. Bailey, ed.). *Rev. Mineral.* **13**, 299-356.

STEPHENSON, D. (1972): Alkali clinopyroxenes from nepheline syenites of the South Qôroq Centre, South Greenland. *Lithos* **5**, 187-201.

STRECKEISEN, A. (1976): To each plutonic rock its proper name. *Earth Sci. Rev.* **12**, 1-33.

SUTCLIFFE, R.H., SMITH, A.R., DOHERTY, W. & BARNETT, R.L. (1990): Mantle derivation of Archean amphibole-bearing granitoid and associated mafic rocks: evidence from the southern Superior Province, Canada. *Contrib. Mineral. Petrol.* **105**, 255-275.

THOMPSON, R.N. (1974): Some high-pressure pyroxenes. *Mineral. Mag.* **39**, 768-787.

TUTTLE, O.F. & BOWEN, N.L. (1958): Origin of granite in the light of experimental studies in the system $NaAlSi_3O_8$–$KAlSi_3O_8$–SiO_2–H_2O. *Geol. Soc. Am., Mem.* **74**.

TYLER, R.C. & KING, B.C. (1967): The pyroxenes of the alkaline igneous complexes of eastern Uganda. *Mineral. Mag.* **36**, 5-21.

UPTON, B.G.J. (1960): The alkaline igneous complex of Kûngnât Fjeld, South Greenland. *Meddr. Grønl.* **123**, 5-145.

VARET, J. (1969): Les pyroxènes des phonolites du Cantal (Auvergne, France). *Neues Jahrb. Mineral., Monatsh.*, 174-184.

WHELLER, G.E., VARNE, R., FODEN, J.D. & ABBOTT, M.J. (1987): Geochemistry of Quaternary volcanism in the Sunda – Banda arc, Indonesia, and three-component genesis of island arc basaltic magmas. *J. Volcan. Geotherm. Res.* **32**, 137-160.

WONES, D.R. & EUGSTER, H.P. (1965): Stability of biotite: experiment, theory, and application. *Am. Mineral.* **50**, 1228-1272.

WOOLLEY, A.R., PLATT, R.G. & EBY, G.N. (1996): Relatively aluminous alkali pyroxene in nepheline syenites from Malawi: mineralogical response to metamorphism in alkaline rocks. *Can. Mineral.* **34**, 423-434.

WYMAN, D. & KERRICH, R. (1989): Archean shoshonitic lamprophyres associated with Superior Province gold deposits: distribution, tectonic setting, noble metal abundances, and significance for gold mineralization. *Econ. Geol., Monogr.* **6**, 651-667.

YAGI, K. (1966): The system acmite – diopside and its bearing on the stability relations of natural pyroxenes of the acmite – hedenbergite – diopside series. *Am. Mineral.* **51**, 976-1000.

YODER, H.S. & TILLEY, C.E. (1962): Origins of basalt magmas: an experimental study of natural and synthetic rock systems. *J. Petrol.* **3**, 342-532.

ZEN, E-AN (1986): Aluminum enrichment in silicate melts by fractional crystallization: some mineralogic and petrographic constraints. *J. Petrol.* **27**, 1095-1117.

Received March 11, 1997, revised manuscript accepted December 20, 1997.